

## Observation of Chaotic Behavior in an Electron-Hole Plasma in Ge

G. A. Held and Carson Jeffries

*Department of Physics and Materials and Molecular Research Division, Lawrence Berkeley Laboratory,  
University of California, Berkeley, California 94720*

and

E. E. Haller

*Department of Materials Science and Mineral Engineering and Lawrence Berkeley Laboratory,  
University of California, Berkeley, California 94720  
(Received 28 November 1983)*

Spontaneous current oscillations which develop chaotic behavior are reported for an electron-hole plasma in a crystal of Ge at 77 K in parallel electric and magnetic fields. The observed behavior includes a period-doubling route to chaos with increasing applied electric field, regions of broadband noise which contain noise-free periodic windows, and bifurcations from quasiperiodic states to turbulence. A rate-equation model, which includes nonlinear coupling between unstable and damped plasma density waves, is presented.

PACS numbers: 72.30.+q, 05.40.+j, 47.25.-c, 52.35.-g

Semiconductor plasmas are of interest both as a medium for wave propagation in solids and as relatively simple models for some gas plasmas. The possibility that plasmas could exhibit chaotic behavior has been discussed theoretically,<sup>1,2</sup> but as yet no clear data for gaseous or solid-state plasmas has been given. We report here such behavior in an electron-hole (e-h) plasma in a crystal of Ge in applied dc electric and magnetic fields. Our system is a continuum (with many degrees of freedom), yet it exhibits low-dimensional behavior such as the period-doubling and the Ruelle-Takens-Newhouse (quasiperiodic) routes to chaos.<sup>3</sup> Chaotic behavior has been observed in many physical systems,<sup>4-6</sup> but prior to this work, the only experimental systems known to follow the Ruelle-Takens-Newhouse route to chaos were hydrodynamic: Couette-Taylor flows and Rayleigh-Bénard convection.<sup>4</sup>

Ivanov and Ryvkin<sup>7</sup> reported the onset of spontaneous coherent current oscillations in a Ge crystal placed in parallel electric and magnetic fields. This instability, the so-called "oscillistor" effect, was subsequently studied in other semiconductors<sup>8</sup>; spontaneous oscillations were only observed in the presence of both electrons and holes. Theoretical models<sup>9,10</sup> attributing these oscillations to a screw-shaped helical instability within the e-h plasma were developed and confirmed experimentally.<sup>11</sup> To study the possible chaotic dynamics of this system, we cut  $1 \times 1 \times 10$ -mm<sup>3</sup> samples from a large single crystal of Ge with a net donor concentration of  $3.7 \times 10^{12}$  cm<sup>-3</sup>. A Li-diffused  $n^+$  contact (electron injecting) and a B-implanted  $p^+$  contact (hole

injecting) were formed on opposite  $1 \times 1$ -mm<sup>2</sup> ends. The sample was lapped, etched, and then stored for 72 h in dry air to allow the surfaces to passivate.

Our experiments are performed by cooling the sample to 77 K in liquid N<sub>2</sub> and connecting it in series with a 100-Ω resistance  $R$  and a variable dc voltage  $V_0$ . A 4-kG magnetic field  $\vec{B}_0$  is applied parallel ( $\pm 3^\circ$ ) to the length of the sample and hence parallel to the applied electric field  $\vec{E}_0$ . Data are taken by increasing the control parameter  $V_0$  from 0 to  $\sim 25$  V and recording the current  $I(t)$  through the sample and the voltage  $V(t)$  across it. The overall behavior of  $I$  is found to be as follows: For  $V_0 < 6$  V,  $I$  has only a dc component. At  $V_0 = 6$  V,  $I$  spontaneously becomes periodic. Regions of chaotic dynamics occur in the intervals  $7.0 \leq V_0 \leq 7.4$  V;  $10.0 \leq V_0 \leq 10.7$  V; and  $14.9 \leq V_0 \leq 18$  V; otherwise,  $I$  is periodic.

The clearest chaotic sequence is shown starting in Fig. 1(a) at  $V_0 = 10.0$  V:  $I(t)$  is oscillating at a fundamental frequency  $f_0 \approx 118$  kHz, i.e., at period 1. The phase portrait,  $I(t)$  vs  $V(t)$ , in Fig. 1(a), shows that the oscillation has a small spectral component at a *harmonic* of  $f_0$ . However, there is no *subharmonic* component, as seen in the power spectrum of  $I(t)$  of Fig. 1(a). As  $V_0$  is increased,  $I(t)$  shows a period-doubling bifurcation; the data shown in Fig. 1(b) display the emergence of a spectral component at  $f_0/2$ . At larger  $V_0$ , another period-doubling bifurcation occurs [Fig. 1(c)] with new spectral components at  $f_0/4$ ,  $3f_0/4$ ,  $5f_0/4, \dots$ . At slightly larger  $V_0$ ,  $I(t)$  becomes nonperiodic [Fig. 1(d)], and its power spectrum enters a region

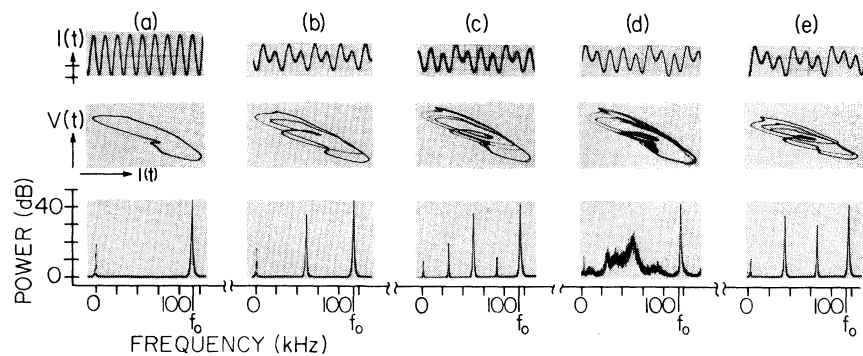


FIG. 1. Oscillatory current,  $I(t)$ ; phase portrait,  $I(t)$  vs  $V(t)$ ; and power spectra of  $I(t)$  for  $1 \times 1 \times 10\text{-mm}^3$  Ge crystal. Applied voltage,  $V_0$ , increasing from (a) to (e) (see Fig. 3).  $I(t)$  scales are 8 sec/div and 0.05 mA/div. Power spectra measured with scanning spectrum analyzer with 60-dB rejection.  $I(t)$  in this and all subsequent figures (except phase portraits) is ac coupled and filtered to remove harmonic distortion.

of broadband noise. For further increases of  $V_0$  there appear noise-free windows of periods 3, 4, 5,  $\dots$ , within this region of broadband noise; see Fig. 1(e) for period 3. This sequence ends at  $V_0 = 10.7$  V with a return to period-1 oscillations.

Figure 2 is a bifurcation diagram, a plot of the local current maxima  $I_{\max}$  vs  $V_0$ . The period-doubling route to chaos as well as the noise-free windows can be clearly seen. A similar sequence of windows has been observed in chemical oscillators<sup>4</sup> and driven  $p$ - $n$  junctions.<sup>12</sup> We have found a finite-difference equation of the form  $I_{n+1} = F(V_0, I_n)$  that also yields such a sequence. We note that the above data are representative and that although spontaneous oscillations and chaotic behavior were observed over a wide range of parameter values, the value of  $f_0$  and the order of a specific sequence is sensitive to the value of the magnetic field and its orientation.

The regions of chaos correspond to motion on a strange attractor in phase space. Figure 3(a) is an observed return map, a plot of all pairs of points  $(I_n, I_{n+1})$  where  $\{I_n\}$  is the set of local current maxima, taken in the chaotic region just beyond the period 3 window. That this map does not fill an entire area in two-dimensional space indicates that the motion is on an attractor of low ( $< 3$ ) dimension.<sup>13</sup>

Another Ge sample, similar to the first, but with dimensions  $3 \times 1 \times 10\text{ mm}^3$ , was observed to exhibit the Ruelle-Takens-Newhouse<sup>3</sup> route to chaos. When it was placed in a 4.3-kG magnetic field approximately parallel to the applied electric field, with  $V_0$  set at 58 V, the current oscillated at a fundamental frequency,  $f_0 = 50$  kHz, with subharmonics  $f_0/3$  and  $2f_0/3$ . When  $V_0$  was increased slightly, the system bifurcated to a quasiperiodic state: oscil-

lation at two incommensurate frequencies, in this case  $f_0 = 50$  kHz and  $f_0 = 3.4$  kHz. Sums and differences of the form  $mf_0/3 + nf_1$  ( $m$  and  $n$  integers) were observed in the power spectrum. As  $V_0$  was increased still further, the power spectrum exhibited broadband noise. Return maps of the system in the quasiperiodic and subsequent non-periodic states are shown in Figs. 3(b) and 3(c). The latter can be seen to fill an entire region of the two-dimensional phase space. This behavior is similar to that of a Couette-Taylor flow at the onset of high ( $> 3$ ) dimensional turbulence.<sup>14</sup> Measurements of the attractor dimensions<sup>15</sup> are in progress.

An experiment similar to the above was done on a  $1 \times 1 \times 10\text{-mm}^3$  sample with Ohmic contacts

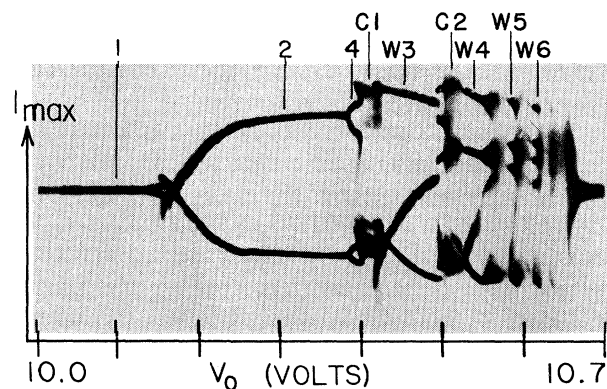


FIG. 2. Bifurcation diagram of local current maxima,  $I_{\max}$ , vs applied voltage,  $V_0$ , for same sample as in Fig. 1. Labels (1), (2), (4), (C1), and (W3) refer to regions displayed in Figs. 1(a) to 1(e), respectively. Labels (W4), (W5), and (W6) refer to noise-free windows of periods 4, 5, and 6, respectively.

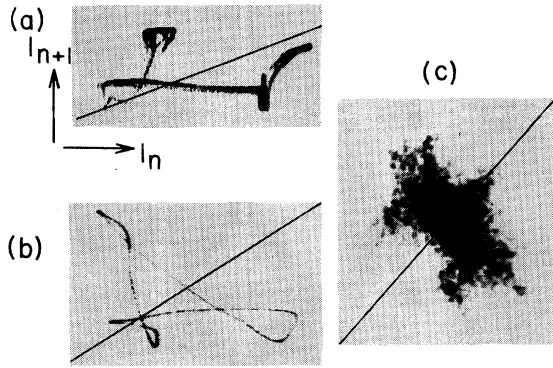


FIG. 3. (a) Return map,  $I_{n+1}$  vs  $I_n$ , where  $\{I_n\}$  is the set of local current maxima, for same sample as in Fig. 1. Return map is shown for region C2 in Fig. 2. Also shown is the line  $I_n = I_{n+1}$ . (b) Return map for  $1 \times 3 \times 10$ -mm<sup>3</sup> Ge crystal with applied voltage  $V_0 = 58.6$  V. (c) Same as (b) except  $V_0 = 58.7$  V, after onset of turbulence.

(which inject only electrons) on both ends; no oscillations or chaotic dynamics were observed. However, when this sample is optically pumped with a 10-mW He-Ne laser at 6328 Å (creating both electrons and holes), current oscillations and period doubling to chaos are observed. This indicates that the observed behavior is a property of the e-h plasma and not dependent on the specifics of carrier production; this is consistent with oscillistor experiments and theory.<sup>8-10</sup>

For times and distances of interest, the following partial differential equations describe the motion of conduction electrons and holes in the presence of applied electric and magnetic fields<sup>9,10</sup>:

$$\vec{J}_{e,h} = n_{e,h} q \mu_{e,h} \vec{E} \pm \epsilon D_{e,h} \nabla n_{e,h} \mp \mu_{e,h} \vec{J}_{e,h} \times \vec{B}, \quad (1)$$

$$\partial n_{e,h} / \partial t = \pm (1/q) \nabla \cdot \vec{J}_{e,h} + \gamma, \quad (2)$$

$$\nabla \cdot \vec{E} = -q(n_e - n_h) / \epsilon. \quad (3)$$

$$n_{h1} \cong n_{e1} = \sum_{k,m} C_{km}(t) N_{km}(r) \exp(-ikz - im\phi) + \text{c.c.}, \quad (4)$$

$$\psi_1 = \sum_{k,m} C_{km}(t) \Psi_{km}(r) \exp(-ikz - im\phi) + \text{c.c.} \quad (5)$$

Substituting (4) and (5) into (1)–(3) results in a partial differential equation,

$$\partial C_{km} / \partial t = M_{km} C_{km} + \sum_{\substack{k_1, k_2: k_1 + k_2 = k \\ m_1, m_2: m_1 + m_2 = m}} M'_{k_1 k_2 m_1 m_2} C_{k_1 m_1} C_{k_2 m_2} + \sum_{\substack{k_1, k_2: k_1 - k_2 = k \\ m_1, m_2: m_1 - m_2 = m}} M'_{k_1 k_2 m_1 m_2} C_{k_1 m_1} C_{k_2 m_2}^* \quad (6)$$

where  $M$  and  $M'$  are independent of time, and only  $M$  is complex.

The subscript  $e(h)$  and the upper (lower) signs refer to electrons (holes);  $n$  is the carrier density,  $q$  is the magnitude of the electronic charge,  $\mu$  is the mobility,  $D$  is the diffusion constant,  $\epsilon$  is the dielectric constant of the sample,  $\gamma$  is the net generation rate (including bulk recombination),  $J$  is the current density, and  $E$  and  $B$  are the electric and magnetic fields, respectively. At surfaces perpendicular to the applied electric field, these equations are subject to the boundary condition  $J_{e\perp} = J_{h\perp} = qsn_e$ , where  $s$  is the surface recombination rate.

By expansion of the carrier densities and the electric field about their equilibrium values

$$\begin{aligned} [n_e = n_{e0} + n_{e1}(t), \quad n_h = n_{h0} + n_{h1}(t), \\ E = E_0 - \nabla \psi_1(t)], \end{aligned}$$

and substitution of these expressions into (1)–(3), it has been shown<sup>9,10</sup> that the first-order terms lead to a helical density wave,

$$n_{h1} \cong n_{e1} = N_1(r) \exp[i\omega t - ikz - im\phi]$$

and

$$\psi_1 = \Psi_1(r) \exp[ij\omega t - ikz - im\phi],$$

as a solution to (1)–(3);  $m$  is an integer. Further, beyond certain thresholds of the applied electric and magnetic fields, this helical density wave is absolutely unstable [ $\text{Im}(\omega) < 0$ ] and spontaneous oscillations occur. Using microwave probes, Misawa and Yamada<sup>11</sup> have observed this helical density wave in an oscillistor. Hurwitz and McWhorter<sup>10</sup> observed experimentally that the onset of spontaneous oscillations coincided with the onset of nonlinear behavior.

To incorporate this nonlinear behavior more readily into a model which explains the observed chaotic dynamics, we consider a *superposition* of waves in which the time dependence is not assumed to be periodic. That is, we assume a solution of the form

Equation (6) describes a wave-wave<sup>16</sup> interaction in which a wave with wave vector  $k$  can couple nonlinearly to many different pairs of waves  $(k_1, m_1)$ ,  $(k_2, m_2)$ . Wersinger, Finn, and Ott<sup>1</sup> numerically studied the evolution of an undamped wave, which is coupled to two damped waves (with equal damping constants  $\Gamma$ ), by equations similar to (6). As  $\Gamma$  is increased, the amplitude of the undamped wave undergoes a period-doubling cascade to a two-dimensional chaotic attractor. Within the chaotic regime a period-3 window is found.

We propose that the chaotic behavior in our system is due to a similar coupling, with the unstable "oscillistor" wave coupling to pairs of damped waves. If one assumes a wave vector on the order of  $1 \text{ cm}^{-1}$  (as was experimentally observed for oscillistors with dimensions comparable to our samples<sup>12</sup>) and considers only the first-order terms in (6), then our fundamental frequency is on the order of  $(1/2\pi) \text{Im}(M_{km}) = \mu_e E_0 k / 2\pi \approx 70 \text{ kHz}$ . Further, our observation of attractors of dimension  $> 2$  indicates a possible coupling between a large ( $> 3$ ) number of waves. Information about the spatial distribution of free carriers in the sample will be essential in determining the validity of this model.

In conclusion, we have observed chaotic behavior in an electron-hole plasma in a Ge crystal. This behavior includes spontaneous current oscillations which exhibit a period-doubling route to chaos, broadband noise, noise-free periodic windows, and bifurcations from quasiperiodic states to turbulence. We have proposed a nonlinear wave-wave coupling model to explain the observed behavior.

We wish to thank J. Hansen, A. Kaufman, M. Lieberman, and J. Crutchfield for helpful discussions, and P. Luke and N. Haegel for assistance in preparing the samples. This work was supported by the Director, Office of Energy Research, Office of Basic Energy Science, Materials Science Division of

the U. S. Department of Energy under Contract No. DE-AC03-76SF00098. One of us (C.D.J.) thanks the Miller Institute for Basic Research in Science for support.

<sup>1</sup>J.-M. Wersinger, J. M. Finn, and E. Ott, *Phys. Fluids* **23**, 1142 (1980).

<sup>2</sup>J. C. Adam, M. N. Bussac, and G. Laval, in *Intrinsic Stochasticity in Plasmas*, edited by G. Laval and D. Grésillon (Les Editions de Physique Courtaouef, Orsay, France, 1979), p. 415.

<sup>3</sup>J.-P. Eckmann, *Rev. Mod. Phys.* **53**, 643 (1981).

<sup>4</sup>For a review of chaotic behavior in physical systems, see H. L. Swinney, *Physica (Utrecht)* **7D**, 3 (1983).

<sup>5</sup>J. Testa, J. Perez, and C. Jeffries, *Phys. Rev. Lett.* **48**, 714 (1982).

<sup>6</sup>S. W. Teitsworth, R. M. Westervelt, and E. E. Haller, *Phys. Rev. Lett.* **51**, 825 (1983).

<sup>7</sup>I. L. Ivanov and S. M. Ryvkin, *Zh. Tekh. Fiz.* **28**, 774 (1958) [*Sov. Phys. Tech. Phys.* **3**, 722 (1958)].

<sup>8</sup>R. D. Larrabee and M. C. Steele, *J. Appl. Phys.* **31**, 1519 (1960); R. D. Larrabee, *J. Appl. Phys.* **34**, 880 (1963); J. Bok and R. Veilex, *Compt. Rend.* **248**, 2300 (1958).

<sup>9</sup>M. Glicksman, *Phys. Rev.* **124**, 1655 (1961); M. Shulz, *Phys. Status Solidi* **25**, 521 (1968).

<sup>10</sup>C. E. Hurwitz and A. L. McWhorter, *Phys. Rev.* **134**, A1033 (1964).

<sup>11</sup>T. Misawa and T. Yamada, *Jpn. J. Appl. Phys.* **2**, 19 (1963).

<sup>12</sup>J. Perez, C. Jeffries, and J. Testa, *Bull. Am. Phys. Soc.* **28**, 383 (1983); S. D. Bronson, D. Dewey, and P. S. Linsay, *Phys. Rev. A* **28**, 1201 (1983).

<sup>13</sup>N. H. Packard, J. P. Crutchfield, J. D. Farmer, and R. S. Shaw, *Phys. Rev. Lett.* **45**, 712 (1980).

<sup>14</sup>A. Brandstätter *et al.*, *Phys. Rev. Lett.* **51**, 1442 (1983).

<sup>15</sup>See, for example, J. D. Farmer, E. Ott, and J. A. Yorke, *Physica (Utrecht)* **7D**, 153 (1983).

<sup>16</sup>R. Z. Sagdeev and A. A. Galeev, *Nonlinear Plasma Theory* (Benjamin, New York, 1969).

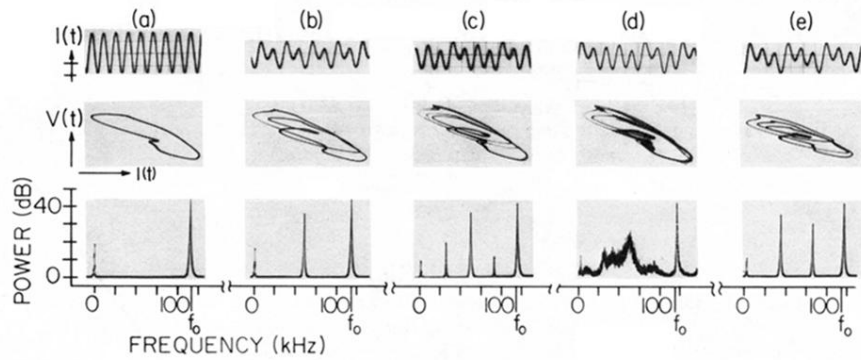


FIG. 1. Oscillatory current,  $I(t)$ ; phase portrait,  $I(t)$  vs  $V(t)$ ; and power spectra of  $I(t)$  for  $1 \times 1 \times 10\text{-mm}^3$  Ge crystal. Applied voltage,  $V_0$ , increasing from (a) to (e) (see Fig. 3).  $I(t)$  scales are 8 sec/div and 0.05 mA/div. Power spectra measured with scanning spectrum analyzer with 60-dB rejection.  $I(t)$  in this and all subsequent figures (except phase portraits) is ac coupled and filtered to remove harmonic distortion.

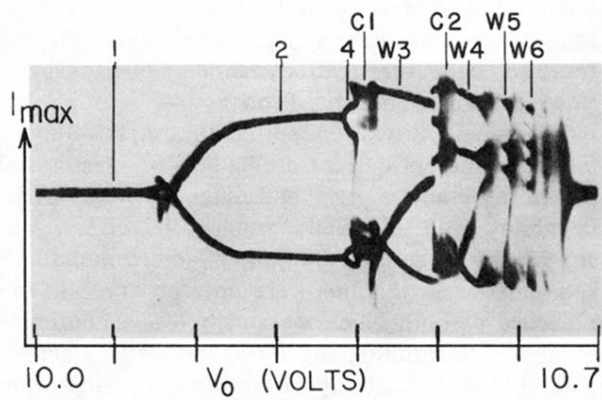


FIG. 2. Bifurcation diagram of local current maxima,  $I_{\max}$ , vs applied voltage,  $V_0$ , for same sample as in Fig. 1. Labels (1), (2), (4), (C1), and (W3) refer to regions displayed in Figs. 1(a) to 1(e), respectively. Labels (W4), (W5), and (W6) refer to noise-free windows of periods 4, 5, and 6, respectively.

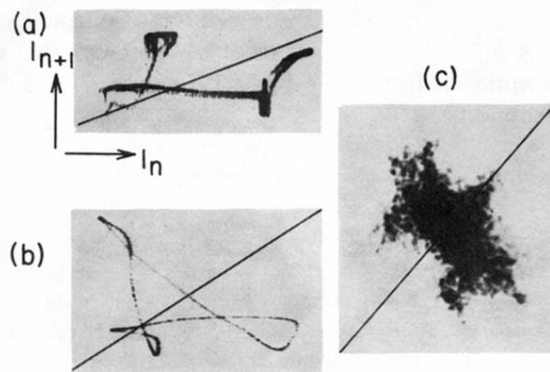


FIG. 3. (a) Return map,  $I_{n+1}$  vs  $I_n$ , where  $\{I_n\}$  is the set of local current maxima, for same sample as in Fig. 1. Return map is shown for region C2 in Fig. 2. Also shown is the line  $I_n = I_{n+1}$ . (b) Return map for  $1 \times 3 \times 10\text{-mm}^3$  Ge crystal with applied voltage  $V_0 = 58.6$  V. (c) Same as (b) except  $V_0 = 58.7$  V, after onset of turbulence.